Support for a three-dimensional structure predicting a Cys-Glu-Lys catalytic triad for *Pseudomonas aeruginosa* amidase comes from site-directed mutagenesis and mutations altering substrate specificity

Carlos NOVO*†[1], Sebastien FARNAUD‡, Renée TATA‡, Alda CLEMENTE* and Paul R. BROWN‡

*Unidade de Tecnologica de Proteínas e Anticorpos Monoclonais, Departmento de Biotecnologia, Instituto Nacional de Engenharia e Tecnologia Industrial, Edifício F, Estrada do Paço do Lumiar 1649-038, Lisbon, Portugal, †Centro de Malária e outras Doenças Tropicais, Instituto de Higiene e Medicina Tropical, Rua da Junqueira 96, 1349-008 Lisbon, Portugal, and ‡Randall Centre for Molecular Mechanism of Cell Functions, King's College London, New Hunt's House, St Thomas Street, London SE1 1UL, U.K.

The aliphatic amidase from *Pseudomonas aeruginosa* belongs to the nitrilase superfamily, and Cys^{166} is the nucleophile of the catalytic mechanism. A model of amidase was built by comparative modelling using the crystal structure of the worm nitrilase–fragile histidine triad fusion protein (NitFhit; Protein Data Bank accession number 1EMS) as a template. The amidase model predicted a catalytic triad (Cys-Glu-Lys) situated at the bottom of a pocket and identical with the presumptive catalytic triad of NitFhit. Three-dimensional models for other amidases belonging to the nitrilase superfamily also predicted Cys-Glu-Lys catalytic triads. Support for the structure for the *P. aeruginosa* amidase came from site-direct mutagenesis and from the locations of amino acid residues that altered substrate specificity or binding when mutated.

Key words: comparative modelling, NitFhit, nitrilase.

INTRODUCTION

Amidases can be assigned to phylogenetically unrelated families on the basis of amino acid sequence. One family comprises the amidase signature group, which includes the amidases from *Aspergillus oryzae* (Swiss-Prot accession number Q12559) [1] and the putative amidase from *Salmonella typhimurium* (Swiss-Prot accession number P33772) [2]. The amidases from *Pseudomonas aeruginosa* (Swiss-prot accession number P11436) [3], *Rhodococcus erythropolis* (Swiss-Prot accession number Q01360) [4], *Helicobacter pylori* (Protein Identification Resource accession number F64556) [5] and *Bacillus stearothermophilus* (EMBL accession number AAF14257) [6] are included in the second branch of the nitrilase superfamily [7]. The amidase from *Mycobacterium smegmatis* (Swiss-Prot accession number Q07838) [8] is included in the urease group.

Nitrilases are thiol enzymes involved in nitrile degradation, converting nitriles directly into the corresponding carboxylic acid plus ammonia through a tetrahedral intermediate, without the intermediate formation of an amide [9]. Nitrilase activity has been reported in bacteria [10], fungi [11,12], plants [12], and recently, *nit* genes were described as fusion proteins with the nucleotide-binding protein fragile histidine triad, NitFhit (nitrilase–fragile histidine triad fusion protein), in invertebrates [13] and in mice and humans [14]. In the amidases belonging to the nitrilase superfamily, an invariant cysteine residue was reported to act as the nucleophile in the catalytic mechanism [15,16], and this was confirmed by site-directed mutagenesis of Cys^{166} in the *P. aeruginosa* amidase [17]. Crystals of the amidase from *P. aeruginosa* have been obtained [17]; however, no three-dimensional (3-D) structure has been described. Recently, the 3-D structure of the nitrilase domain of NitFhit from the worm was reported [14], and the putative catalytic triad Cys-Glu-Lys was shown to be conserved in all members of the nitrilase superfamily [7].

The substrate specificity of the *P. aeruginosa* amidase encoded by the *amiE* gene is limited to short aliphatic amides, but has been extended through a variety of point mutations to include longer aliphatic amides, such as butyramide [18,19], valeramide [18] and aromatic amides, acetanilide [20] and phenylacetamide [21]. In the mutant strain AI3, the *amiE* mutation $Thr^{103} \rightarrow Ile$ is responsible for the amidase activity towards acetanilide [20]. Urea and hydroxyurea are active-site-directed inhibitors of *P. aeruginosa* amidase and additional mutations in the *amiE* gene of strain AI3 that result in decreased binding affinity of amidase for urea have been identified ($Arg^{188} \rightarrow$ Cys, His or Leu; $Gln^{190} \rightarrow Glu$; and $Trp^{144} \rightarrow Cys$) [22].

In the present study, a model for the core structure of the *P. aeruginosa* amidase has been constructed and some of the residues implicated in catalysis have been investigated by site-directed mutagenesis. Validation of the model has also been sought from the locations of mutations that alter the substrate specificity of amidase and mutations that reduce its binding affinity for urea.

EXPERIMENTAL

Comparative modelling

The Fast Automatic Modelling System ('FAMS') server [23–25] and the automated knowledge-based protein modelling server SwissModel v.3.5 [26–29] for comparative modelling were used. Procheck v.3.4 for Windows NT [30] was used for model validation. Root mean square ('RMS') value calculations between the model and the templates used for comparative modelling, using the Cα fitting, were performed by using the Swiss-PdbViewer v3.7b2 [28]. Topology search and comparison

Abbreviations used: 3-D, three-dimensional; NitFhit, nitrilase–fragile histidine triad fusion protein; PNA, *p*-nitroacetanilide; SSE, secondary structure element.

[1] To whom correspondence should be addressed (e-mail carlos.novo@ineti.pt).

The co-ordinates for the structure of the *Pseudomonas aeruginosa* amidase fragment (residues 20–290) have been deposited in the Protein Data Bank under accession number 1K17.

Table 1 *P. aeruginosa* strains used or referred to in this study

Abbreviations used: AI, acetanilide; C, carbon; N, nitrogen; OHU, hydroxyurea; U, urea.

Strain	Parent	Selection medium (C/N sources)	Reference
8602 (PAC 1)*			[37]
L10 (PAC 142)	8602	Succinate/lactamide	[38]
AI3 (PAC 366)	L10	AI/N	[20]
3B	L10	AI/N	This study
8A	L10	AI/N	This study
10A	L10	AI/N	This study
11A	L10	AI/N	This study
8AOH1	8A	AI/N/OHU	This study
10AAU1	10A	AI/N/U	This study
10AAU3	10A	AI/N/U	This study

* PAC 1 is the wild-type strain.

was done using the server TOPS [31]. Distribution of low-energy ligand positions in the proximity of the binding site of the protein was calculated at low resolution (4.5 Å, where 1 Å = 0.1 nm), using the Global Range Molecular Matching ('GRAMM') program [32–35]. The catalytic pocket was predicted using the WHAT IF program through the World Wide Web interface [36].

Bacterial growth and mutant isolation

The origins of the bacterial strains [20,37,38] are shown in Table 1. For growth of broth cultures, Oxoid No. 2 broth was used for *Pseudomonas* strains and Luria–Bertani broth for growth of *Escherichia coli* strains. For isolation of urea- and hydroxyurea-resistant mutants, 0.05% (w/v) urea or 0.05% (w/v) hydroxyurea was added to acetanilide solid medium {1% (w/v) Noble agar (Difco Laboratories, Detroit, MI, U.S.A.) containing minimal salts medium [40] supplemented with 0.1% (w/v) acetanilide and 0.1% (w/v) ammonium sulphate as the carbon and nitrogen sources respectively}.

For growth of *Pseudomonas* strains for amidase purification, lactate medium [minimal salts medium containing 0.3% (w/v) sodium lactate and 0.1% (w/v) ammonium sulphate as the carbon and nitrogen sources respectively] was used. Acetanilide-utilizing mutants were isolated by plating 50 μl of an overnight broth culture of strain L10 on to acetanilide solid medium and incubating at 37 °C. After 7 days, colonies were picked and restreaked on to the isolation medium to purify them.

Amidase activity measurements

Activity towards *p*-nitroacetanilide (PNA) was assayed spectrophotometrically by following the formation of 4-nitroaniline at 400 nm [40]. Initial velocity data were fitted to the Michaelis–Menten equation using the Leonora program [41]. Amidase protein concentration was determined as described previously [40].

Amidase purification

Amidase was purified from *P. aeruginosa* in a two-step procedure. Cells grown in 5 litres of lactate medium overnight at 37 °C in a rotary shaker were harvested by centrifugation at 6000 ***g*** for 10 min at 10 °C, washed, re-centrifuged, and the cell pellets were used immediately or stored at −20 °C. Extracts were prepared by re-suspending 1 g of cell wet weight in 4 ml TME buffer [20 mM Tris/1 mM EDTA/1 mM 2-mercaptoethanol (pH 7.2)] and sonicating at 160 W for 1 min/ml on ice. The suspension was centrifuged at 30000 ***g*** for 20 min at 4 °C, and the supernatant was loaded on to a 2 × 10 cm DEAE Sepharose CL 4B column (Amersham Biosciences, Uppsala, Sweden) equilibrated with TME buffer. Proteins were eluted with a 0.1–0.35 M KCl gradient in TME buffer. Fractions with amidase activity were pooled, dialysed against TME at 4 °C and then applied to an acetamide epoxy-activated Sepharose CL 4B column prepared and used as described previously [18]. Amidase was eluted with a linear gradient of 20–100 mM NaCl in TME buffer. Purity was checked by silver staining of SDS/PAGE gels. Purification of amidases from *E. coli* followed the procedure described previously [18].

DNA manipulations and site-directed mutagenesis

DNA manipulations and PCR amplification of the *amiE* gene were carried out as described previously [22]. Site-directed mutagenesis was performed using the Altered Sites protocol (Promega, Madison, WI, U.S.A.). The base substitutions were introduced into the *amiE* gene cloned into pAlter-ex1 using the following mutagenic oligonucleotides: $Lys^{134} \rightarrow Asn$, 5′-GCACCAGGGAATAATATTGCGGTACTTC-3′; $Glu^{59} \rightarrow Gln$, 5′-TGATGCCCTGCAAGCTGTACTGCGGGAACACC-3′; and $Glu^{59} \rightarrow Asp$, 5′-TGATGCCCTGCAAGCTGTAGTCCGGGAACACC-3′. The mutation encoding the $Lys^{134} \rightarrow Arg$ mutation was introduced into the *amiE* gene cloned into pAlter-1 using the mutagenic oligonucleotide 5′-AGAAGGTACCGCAGAATCATTCCCTGG-3′. The altered gene was subcloned into the expression vector pKK233-3. The mutated *amiE* genes were checked by automated DNA sequencing.

RESULTS

Modelling of amidase

Inclusion of selected amidases in the nitrilase superfamily is on the basis of structural alignments showing that there is extensive similarity within five regions between the two groups of enzymes (Figure 1). This formed the basis for comparative modelling of the *P. aeruginosa* amidase (fragment 20–290), which was performed using the NitFhit structure, 1EMS, as a template [14]. More than 80% of non-glycine and non-proline residues have conformational angles (ϕ, ψ) in permitted regions of the Ramachandran plot, 0.9% fall in the 'generous allowed' region, and 1.3% fall in the disallowed region, as defined by Procheck [30]. All glycine residues are in permitted regions and one proline is in a disallowed region. The root mean square value between the model and the template used for comparative modelling is 0.38 Å for 255 Cα atoms.

The nitrilase domain of 1EMS spans from residues 10–296 [13], comprising five α-helices and 13 β-strands. Nitrilase can be assigned to the α/β class and the four-layer sandwich architecture. Twelve β-strands, secondary structure element (SSE) numbers 21, 20, 17, 15, 12, 11, 22, 1, 3, 5, 6 and 7 participate in the layer sandwich. Four extra β-strands form two anti-parallel β-sheets (SSE numbers 9–8 and 19–18). Topological comparison with the model constructed for the amidase (Protein Data Bank accession number 1K17) showed that it lacks the β-strands equivalent to β-strands SSE numbers 8, 9 and 11 of 1EMS (Figure 2). The absence of a β-strand, equivalent to SSE number 1 from 1EMS in the amidase model, is probably because the model starts at residue 20. We conclude that amidase has a layer sandwich comprising 11 β-strands equivalent to the layer sandwich in the 1EMS structure. The amidase shows an extra β-sheet identical with the β-sheet in 1EMS formed by SSE 19–18. These results

```
1EMS        10  MATGRHFIAV CQM-----TS DNDLEKNFQA AKNMIE---- -RAGE--KK-
P11436      20         YKM PRL-----HT AAEVLDNARK IADMIV---- -GMKQ--GLP
Q01360      15         VAV VNYK---MPR LHDRAGVLEN ARKIADMMIG MKTGL--PG-
F64556       6         YKM PRL-----HT KNEVLENCRN IAKVIG---- -GVKQGLPG-
AAF14257     6         VAV VNYKMPRLHT KKEVIENAKN IANMIVG--- MKQGL--PG-

1EMS        47  -CEMVFLPEC F-D-FI-GLN KNEQIDLAMA TDCEYMEKYR E---LARKHN
P11436      51  GMDLVVFPEY S-LQGI-MYD PAEMMETAVA IPGEETEIFS R---ACRKAN
Q01360      52  -MDLVVFPEY S-T-QGIMYN EEEMYATAAT IPGDETAIFS AACREADTWG
F64556      38  -LDLIIFPEY STH-GI-MYD RQEMFDTAAS VPGEETAIFA E---ACKKNK
AAF14257    43  -MDLVIFPEY S-T-MGIMYD RKEMFETATT IPGPETEIFA E---ACRKAN
                      **               *    *
                     ©
1EMS        90  IW--LSLGGL H-HKDPSDAA HPWNTHLIID SDGVTRAEYN KLHLFDLEIP
P11436      96  VW--GVFSLT GERHEEHPRK APYNTLVLID NNGEIVQKYR KIIPWCP---
Q01360      99  IF--SITGEQ H-EDHPNK-- PPYNTLILID NKGEIVQRYR KILPWCP---
F64556      82  VW--GVFSLT G-EKHEQAKK NPYNTLILVN DKGEIVQKYR KILPWCP---
AAF14257    87  TWGVFSLTGE Q-HEEHPHK- NPYNTLVLIN NKGEIVQKYR KIIPWCP---
                                    * **        *     *  *
                                                        ©
1EMS       137  GKVRLMESEF SKAGTEMIPP VDTPIGRLGL SICYDVRFPE LSLWNRKRGA
P11436     141  -------IEG WYPGGQTYVS EGPKGMKISL IICDDGNYPE IWRDCAMKGA
Q01360     141  -------IEG WYPGDTTYVT EGPKGLKISL IICDDGNYPE IWRDCAMKGA
F64556     126  -------IEC WYPGDKTYVV DGPKGLKVSL IICDDGNYPE IWRDCAMRGA
AAF14257   132  -------IEG WYPGDTTYVT EGPKGIKISL IICDDGNYPE IWRDCAMKGA
                      *     *                 *  ** *   **          **
                                                ©
1EMS       187  QLLSFPSAFT LNTGLAHWET LLRARAIENQ CYVVAAAQTG AHNPKRQSYG
P11436     184  ELIVRCQGYM YP-AKDQQVM MAKAMAWANN CYVAVANAAG FDG-VYSYFG
Q01360     184  ELIVRCQGYM YP-AKDQQVM MSKAMAWANN CYVAVANAAG FDG-VYSYFG
F64556     169  ELIVRCQGYM YP-AKEQQIA IVKAMAWANQ CYVAVANATG FDG-VYSYFG
AAF14257   175  ELIVRCQGYM YP-AKEQQIM MAKTMAWANN VYVAVANATG FDG-VYSYFG
                 *                          *  *   **  *   *          *

1EMS       237  HSMVVDPWGA VVAQC-SERV DMCFAEIDLS YVDTLREMQP VFSHRRSDLY
P11436     232  HSAIIGFDGR TLGECGEEEM GIQYAQLSLS QIRDARANDQ SQNHLFKILH
Q01360     232  HSAIIGFDGR TLGETGEEEY GIQYAQLSVS AIRDARENDQ SQNHIFKLLH
F64556     217  HSSIIGFDGH TLGECGEEEN GLQYAQLSVQ QIRDARKYDQ SQNQ
AAF14257   223  HSAIIGFDGR TLGECGEEEN GIQYAEISLS QIRDFRQNAQ SQNHLFKLLH
                 **      *         *       *           *

1EMS       286  TLHINEKSSE TGGLKFARFN IPADHIFYST PHSFVFVNLK PVTDGHVLVS
P11436     282  RG---YSGLQ AS
Q01360     282  RGYSGVHAAG DG
F64556
AAF14257   273  RGYTGIIQSG EG
```

Figure 1 Structural alignment of models with the template 1EMS

Structural alignment of NitFhit (1EMS) with *P. aeruginosa* (P11436), *R. erythropolis* (Q01360) *H. pylori* (F64556) and *B. stearothermophilus* (AAF14257) amidases. Residues identical among all structures (* and in bold) and residues participating in the catalytic triad (©) are indicated. Structural alignment was performed using Swiss-PdbViewer v3.7b2.

suggest that amidase from *P. aeruginosa* exhibits a similar folding to 1EMS (Figure 3).

Theoretical models of amidases from *R. erythropolis* (fragment 15–293), *H. pylori* (fragment 15–279) and *B. stearothermophilus* (fragment 6–284) were also constructed by comparative modelling using 1EMS as template (results not shown). These models confirmed the prediction that the nitrilase domain from 1EMS is a template for the core structures of amidases belonging to the nitrilase superfamily.

Amidase active site

Cys^{166} is the nucleophile of the catalytic mechanism of amidase from *P. aeruginosa* [16,17]. In the amidase model (Figure 4), residues Cys^{166}, Glu^{59} and Lys^{134} aligned with those proposed to form a catalytic triad Cys^{169}, Glu^{54} and Lys^{127} in 1EMS, suggesting that amidase has the same catalytic triad. Similar distances (in Å) were observed between equivalent atoms for the catalytic triad of both structures (Figure 4).

Superimposition of all the amidase 3-D models constructed predicts the residues Cys^{166}, Glu^{59} and Lys^{134} for *R. erythropolis*, Cys^{151}, Glu^{45} and Lys^{119} for *H. pylori*, and Cys^{157}, Glu^{50} and Lys^{125} for *B. stearothermophilus* as the catalytic triads for these amidases (results not shown), in agreement with the prediction from the amino acid sequence analysis [7].

Site-directed mutagenesis of putative catalytic triad residues

To investigate the effects of eliminating the charge on Glu^{59} and reducing the size of the side-chain, the mutations $Glu^{59} \rightarrow Gln$ and $Glu^{59} \rightarrow Asp$ were engineered by site-directed mutagenesis. In both cases the resulting amidases were inactive. Both mutant

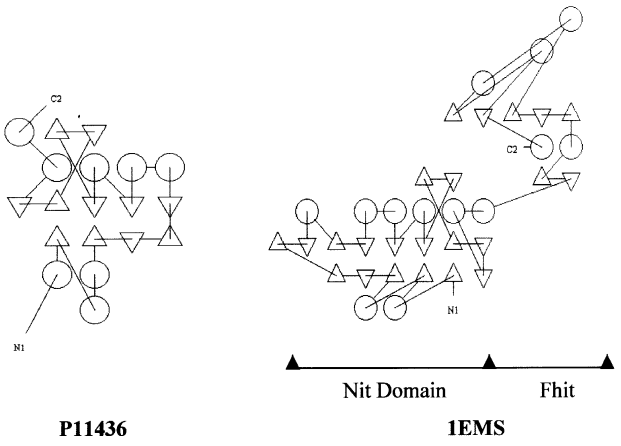

Figure 2 Topology comparison of models

Topology of the *P. aeruginosa* amidase (P11436/1K17) and Nit domain and Fhit of NitFhit (1EMS). Triangular and circular symbols represent β-strands and helices (α and 3_{10}) respectively. Each secondary structure element has a direction (N1 to C2), which is either 'up' (out of the plane of the diagram) or 'down' (into the plane of the diagram). 'Up' strands are indicated by upward pointing triangles and 'down' strands by downward pointing triangles. SSE number of equivalent β-strands of 1EMS and P11436/1K17 respectively, participating in β-sandwich: (1, none), (3, 2), (5, 5), (6, 6), (7, 7), (11, none), (12, 8), (15, 11), (17, 13), (20, 16) and (21, 17); and β-sheet: (8, none), (9, none), (18, 14) and (19, 15).

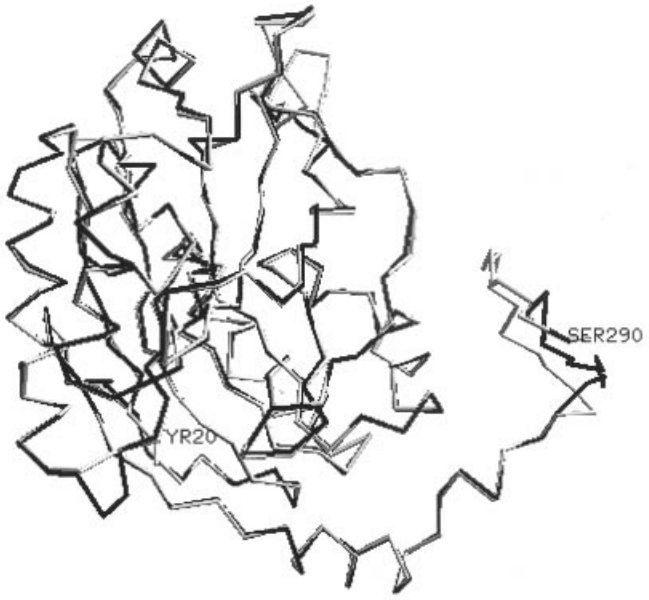

Figure 3 Superimposition of amidase model and 1EMS

Amidase model (1K17; black) and NitFhit (1EMS; grey) are displayed in backbone representation. *P. aeruginosa* numbering was used. Tyr^{20} and Ser^{290} (1K17) are structurally aligned with Ile^{17} and Gly^{297} (1EMS) respectively. The superimposition was generated by Swiss-PdbViewer v3.7b2.

amidases ($Glu^{59} \rightarrow Gln$ and $Glu^{59} \rightarrow Asp$) were identified as the dominant proteins in cell-free extracts by SDS/PAGE (Figure 5); however, only the $Glu^{59} \rightarrow Gln$ amidase was observed by native PAGE, in which it produced a more diffuse band than the native amidase (results not shown).

Site-directed mutagenesis was used to introduce the $Lys^{134} \rightarrow Arg$ mutation. Mutant enzyme was detected as the dominant protein in extracts by SDS/PAGE (Figure 5); however, it proved unstable and was not detected by native PAGE. Activities measured in whole cells showed a 200-fold reduction in activity compared with wild-type enzyme expressed from the same vector. Substitution of Lys^{134} with asparagine produced a stable protein (Figure 5) that had no activity.

Mutations affecting amidase substrate specificity and urea binding

Several acetanilide-utilizing mutant strains were isolated from the constitutive amidase strain L10 and were grouped according to the thermostability and pH profiles of the amidases produced (results not shown). Strains AI3, 3B, 8A and 10A were selected as representatives of different categories of mutant. Their amidases were purified and kinetic parameters determined (Table 2). K_m values for PNA hydrolase activity of the amidases were different in each case. The AI3 enzyme had the lowest k_{cat} value with PNA as substrate. Each amidase had a different catalytic-centre activity with AI3 having the highest followed by 3B > 8A > 10A.

Sequencing performed on the *amiE* genes from the four new strains showed that each one harboured a different mutation: two had point mutations (3B: A at +212 to G, resulting in $Gln^{63} \rightarrow Arg$; and 10A: C at +367 to T, resulting in $Pro^{115} \rightarrow Ser$), one had an insertion (11A: GAG inserted at +235 to +237, resulting in the insertion of Glu^{71}) and one a deletion (8A: GAG deleted at +235 to +237, resulting in the deletion of Glu^{71}). Mutant strains 8AOH1, 10AAU1 and 10AAU3, producing amidases with elevated resistance to urea inhibition, were obtained from two of the acetanilide-utilizing mutant strains, 8A and 10A, and the mutations responsible were determined by sequencing their *amiE* genes: 8AOH1 (C at +586 to T, resulting in $Arg^{188} \rightarrow Cys$); 10AAU1 (C at +586 to T, resulting in $Arg^{188} \rightarrow Cys$); and 10AAU3 (G at +587 to T, resulting in $Arg^{188} \rightarrow Leu$). In each case, Arg^{188} had been substituted and the original mutation responsible for activity towards acetanilide retained.

Pocket model prediction

Analysis of residues participating in the pocket predicted by the WHAT IF program (Figure 6) showed that it included the proposed catalytic triad Glu^{59}, Lys^{134} and Cys^{166}, as well as most of the residues which, after mutation, were associated with substrate specificity for acetanilide (Gln^{63}, Thr^{103} and Pro^{115}) and, in some cases, with low-binding substrate affinity towards urea and hydroxyurea (Trp^{144} and Gln^{190}). The predicted pocket did not include the Glu^{71} (which when deleted or duplicated is associated with acetanilide hydrolase activity) or Arg^{188}, whose substitution caused decreased binding affinity for urea. Superimposition of the pocket and the amidase model (Figure 7) shows that the residues forming the catalytic triad lie at the bottom of the pocket. The sites of mutations, which confer substrate specificity towards acetanilide or low-binding affinity towards urea and hydroxyurea, are located in the loops surrounding the catalytic triad.

Docking results

Low-resolution docking may tolerate structural inaccuracies of the order of 7 Å, which is the precision characteristic of many protein models [42–44]. Low-energy positions of ligands predicted by the Global Range Molecular Matching program [45] tend to cluster in the area of the global minimum, and acetamide docking with the pocket at a resolution of 4.5 Å showed that, of the five predicted lowest energy potential binding places, four are

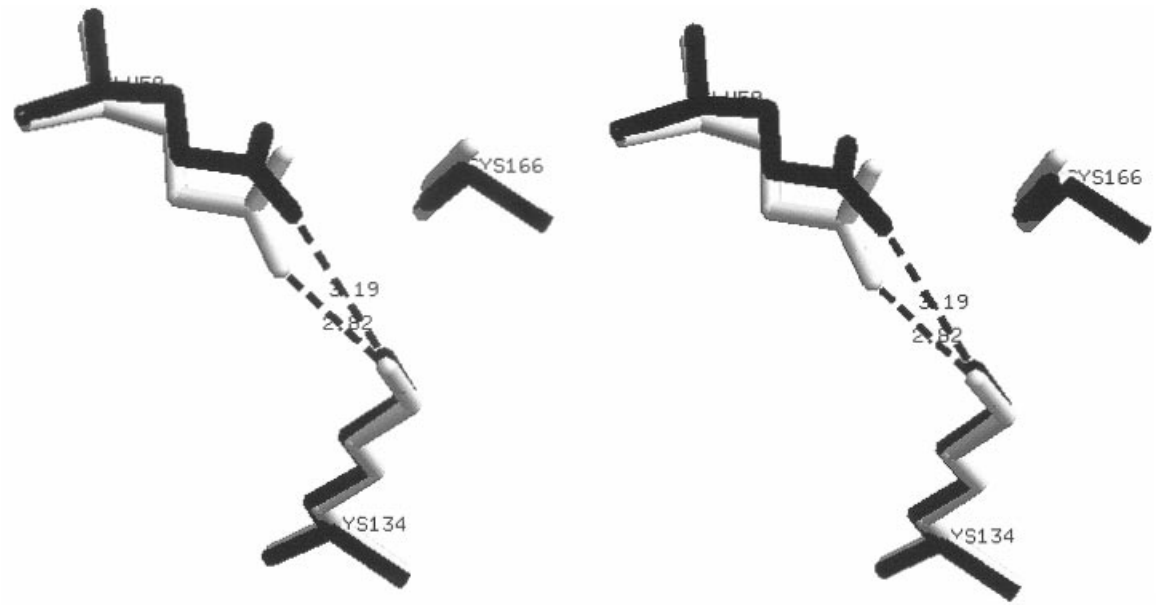

Figure 4 Stereo-view of the structural superimposition of the catalytic triads from the amidase of *P. aeruginosa* (1K17) and 1EMS

Residues from the *P. aeruginosa* amidase (1K17; black) and NitFhit (1EMS; grey) participating in the catalytic triad are shown. H-bonds and distances (in Å) between Lys^{134} and Glu^{59} of 1K17 and Lys^{127} and Glu^{54} of 1EMS are shown. *P. aeruginosa* numbering is used. The Figure was generated by Swiss-PdbViewer v3.7b2.

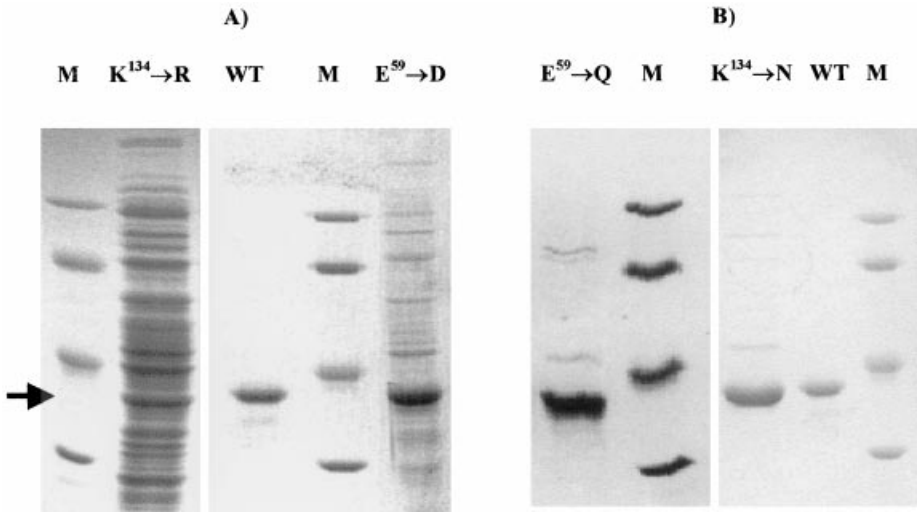

Figure 5 SDS/PAGE analysis

SDS/PAGE of extracts (**A**) and purified amidases (**B**) from cells producing amidases altered by site-directed mutagenesis. M, molecular-mass markers (94 kDa, phosphorylase b; 67 kDa, albumin; 43 kDa, ovalbumin; and 30 kDa, carbonic anhydrase). The arrow denotes the position of amidases. WT, purified wild-type amidase; $K^{134} \rightarrow R$, $Lys^{134} \rightarrow Arg$; $E^{59} \rightarrow D$, $Glu^{59} \rightarrow Asp$; and $K^{134} \rightarrow N$, $Lys^{134} \rightarrow Asn$.

clustered together (Figures 6 and 7). Three of the positions are predicted to be in a similar place in complexes of acetamide with the amidase model, lending support to the proposed catalytic pocket.

DISCUSSION

The results indicate that the *P. aeruginosa* amidase shares a structural and catalytic framework with the nitrilase domain of 1EMS, in which the clustering of the residues Cys^{166}, Glu^{59} and Lys^{134} suggests that they may constitute a catalytic triad. In the amidase model, Cys^{166}, the putative nucleophile, has ϕ and ψ angles which place the residue in a disallowed region of the Ramachandran plot. The same is true for the equivalent cysteine residue in the 1EMS template, which could suggest that substrate binding induces structural adjustments necessary for enhancing the nucleophilicity of Cys^{166}, enabling it to attack the carbonyl carbon of the substrate.

A similar structure (1ERZ, Protein Data Bank accession number) and active-site configuration has been reported for

Table 2 Comparison of the activities of purified amidases towards PNA

It was assumed that [protein] = $[E]_0$ (where $[E]_0$ is the total enzyme concentration). A molecular mass of 230.4 kDa was used (6 × 38.4 kDa). Kinetic parameters were calculated for PNA hydrolysis. k_{cat} was calculated from $k_{cat} = V_{max}/[E]_0$. Results are the means ± S.E.M. estimated by fitting initial velocity data to the Michaelis–Menten equation using the Leonora program [41].

Mutant strain	K_m (mM)	k_{cat} ($\times 10^2$) (s^{-1})	k_{cat}/K_m ($s^{-1} \cdot M^{-1}$)
3B	1.98 ± 0.51	2.80 ± 0.90	11.5
8A	1.17 ± 0.08	0.21 ± 0.04	1.79
10A	0.63 ± 0.20	0.04 ± 0.01	0.63
AI3	0.50 ± 0.04	7.80 ± 0.32	156

carbamyl-D-amino acid amidohydrolase from *Agrobacterium* sp. [46], which, although showing low overall sequence similarity with nitrilases and amidases, nonetheless conserves the residues postulated to be involved in catalysis.

It has been proposed for 1EMS and 1ERZ that the glutamate residue acts as a base by withdrawing a proton from the cysteine residue, thus enhancing its nucleophilicity [14,46]. For 1ERZ, this was postulated to occur either through a direct interaction (on the basis of a distance of < 3 Å in a combination of rotamers of the two side chains) between the glutamate and cysteine residues or indirectly through a water molecule. The putative catalytic triads of 1K17, 1ERZ and 1EMS showed good superimposibilty when structural comparisons were made (results not shown), indicating that a similar role can be postulated for Glu^{59} in amidase. However, site-directed mutagenesis of Glu^{59} resulted not only in loss of enzyme activity, but also in structural changes.

In addition to the substitutions reported in the present study ($Glu^{59} \rightarrow Gln$ and $Glu^{59} \rightarrow Asp$), another change ($Glu^{59} \rightarrow Val$) has been found in an amidase-negative mutant strain [47]. The $Glu^{59} \rightarrow Val$ substitution resulted in dissociation of the hexamer into dimers [47], and examination of the purified $Glu^{59} \rightarrow Gln$ amidase by ultracentrifugation showed that it existed in an equilibrium between hexameric and trimeric states (P. R. Brown and R. L. Beavil, unpublished work). The $Glu^{59} \rightarrow Asp$ substitution apparently caused disaggregation, since the enzyme was not detected by native PAGE. These observations may indicate a role for Glu^{59} in the maintenance of quaternary structure. A hypothesis attributing a simultaneous structural and catalytic role for Glu^{59} may be formulated from previous work [48], which indicated that only one acetamide molecule was bound per hexameric amidase molecule in a catalytic cycle. Conformational changes induced by binding to one subunit were presumed to prevent acetamide binding to the other subunits. Structural changes induced by substrate binding probably have long-distance effects, which could disrupt the quaternary structure of the enzyme if not compensated by subunit–subunit interactions, and the Glu^{59} residues in the other five subunits may have a function in preserving the quaternary structure needed for enzyme activity. The function of Lys^{134} is unknown, but it was speculated [46] that the equivalent lysine residue in carbamyl-D-amino acid amidohydrolase stabilizes the oxyanion of the tetrahedral intermediate through interaction of its ε-NH_2 group with the carbonyl group of the amide substrate. Substitution of Lys^{134} by a similarly charged arginine residue was associated with a large loss of activity, but interpretation was complicated by the instability of the resulting enzyme. Neutralization of the positive charge by replacing Lys^{134} with an asparagine residue did not affect quaternary structure, but eliminated all activity [46]. Early

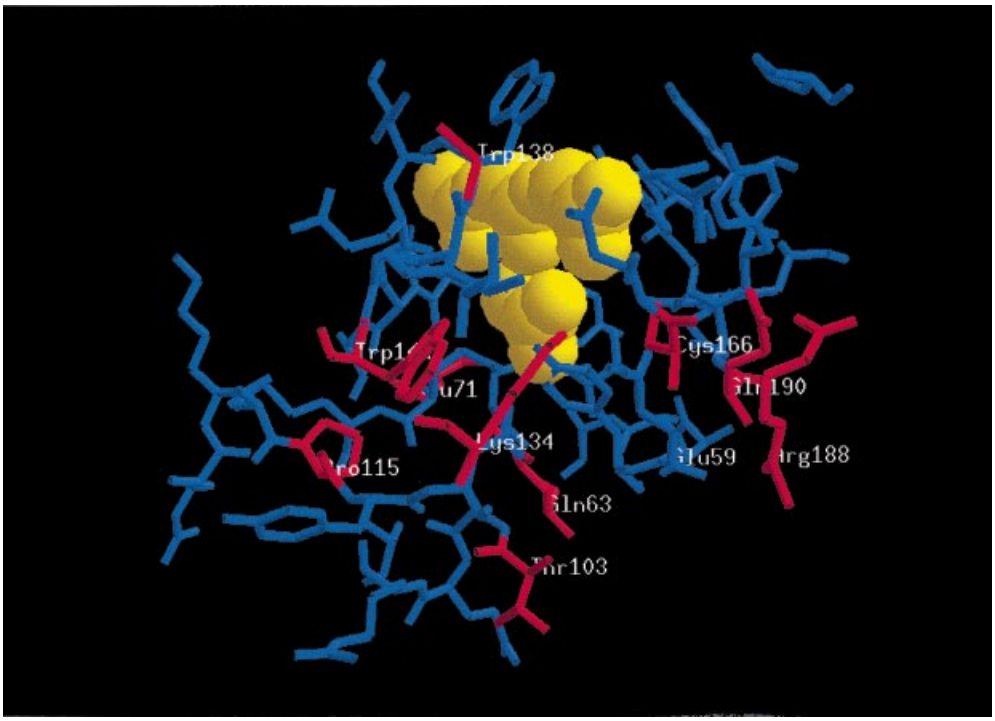

Figure 6 Predicted positions of acetamide molecules inside the amidase pocket

Acetamide–catalytic pocket complex. Catalytic triad and residues involved in substrate specificity alterations are labelled. Acetamide molecules (yellow, spacefill), catalytic pocket residues (blue) and residues involved in substrate specificity alterations (red) are displayed. The Figure was generated by Swiss-PdbViewer v3.7b2.

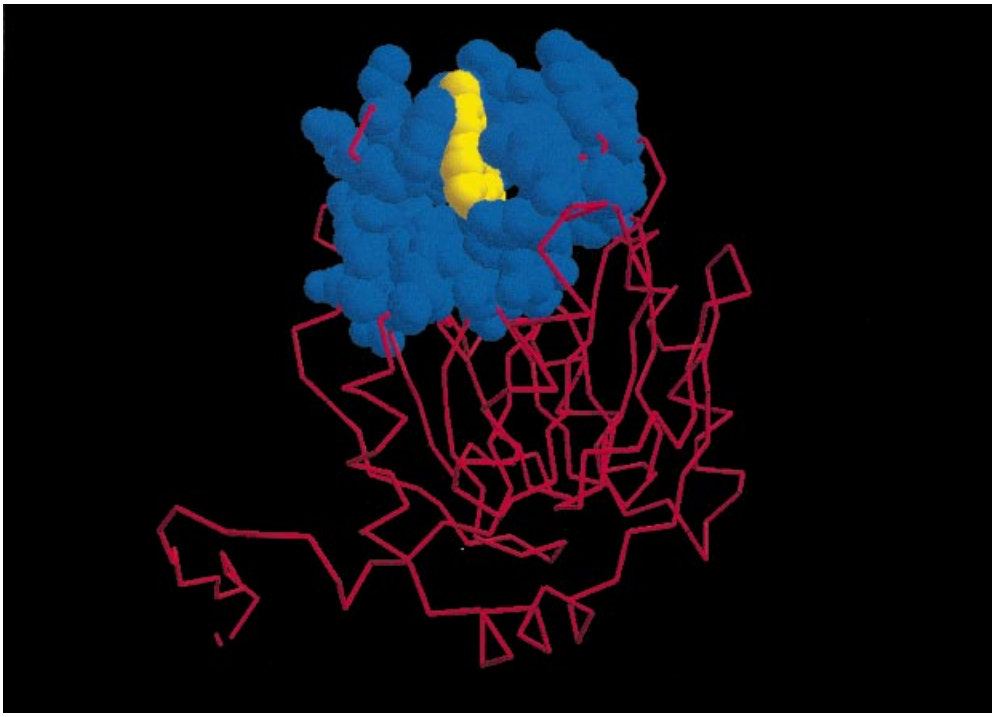

Figure 7 Superimposition of acetamide–pocket complex with the amidase model

Acetamide molecules (yellow) and catalytic pocket residues (blue) are displayed in a spacefill representation. Amidase model residues (red) are displayed in backbone representation. The Figure was generated by Swiss-PdbViewer v3.7b2.

work with amidase to investigate the relationship between kinetic constants and pH also indicated the participation of an unidentified lysine residue contributing to catalysis [49].

The mutations, which result in acquisition of PNA activity, affect amino acid residues that lie within the pocket that harbours the putative triad. Trp^{144} is also present in the pocket, alterations to which result in low-binding affinity towards urea and hydroxyurea [22]. PNA hydrolase activity is associated with deletion of Glu^{71} in strain 8A and with insertion of another glutamate residue adjacent to Glu^{71} in strain 11A. Glu^{71} lies in a region predicted to be α-helical and both mutations alter the direction of the helical dipole moment, implying that they generate alterations in the packing of the helix. The present study shows that substitution of Arg^{188} relieves the inhibitory effect of urea and hydroxyurea on growth on acetanilide medium irrespective of the mutation responsible for the acetanilide specificity and indicates that some of the binding interactions of acetanilide with the enzyme are separate from those of urea. Arg^{188} is not included in the pocket predicted by the WHAT IF program. This may be due to inaccuracies in the model in this region. Trp^{138} also lies in the catalytic pocket and, recently, Karmali et al. [50] showed that the substitution $Trp^{138} \rightarrow Gly$ changed amidase substrate specificity and caused alterations in the stability and conformation of the enzyme. X-ray diffraction analysis of amidase crystals, which is underway, and a more detailed study focused on the pocket–substrate interactions will give a better understanding of the functions of the individual residues and how nitrilases and amidases differ with respect to substrate binding and catalytic mechanism.

We are grateful to Brian J. Sutton (Randall Centre for Molecular Mechanisms of Cell Function, King's College London, London, U.K.) for helpful suggestions. This research was funded by a grant from the Programme Praxis XXI, Science and Technology Foundation, Portuguese Ministry of Scientific Research (project 3/3.1/CEG/2508/95), and a grant from the Biotechnology and Biological Sciences Research Council (29/G12871) to P.R.B.

REFERENCES

1 Gomi, K., Kitamoto, K. and Kumagai, C. (1991) Cloning and molecular characterization of the acetamidase-encoding gene (*amdS*) from *Aspergillus oryzae*. Gene **108**, 91–98
2 Xu, K. and Elliot, T. J. (1993) An oxygen-dependent coproporphyrinogen oxidase encoded by the hemF gene of *Salmonella typhimurium*. J. Bacteriol. **175**, 4990–4999
3 Ambler, R. P., Auffret, A. D. and Clarke, P. H. (1987) The amino acid sequence of the aliphatic amidase from *Pseudomonas aeruginosa*. FEBS Lett. **215**, 285–290
4 Soubrier, F., Levy-Schill, S., Mayaux, J. F., Petre, D., Arnaud, A. and Crouzet, J. (1992) Cloning and primary structure of the wide-spectrum amidase from *Brevibacterium* sp. R312: high homology to the amiE product from *Pseudomonas aeruginosa*. Gene **116**, 99–104
5 Tomb, J. F., White, O., Kerlavage, A. R., Clayton, R. A., Sutton, G. G., Fleischmann, R. D., Ketchum, K. A., Klenk, H. P., Gill, S. P., Dougherty, B. A. et al. (1997) The complete genome sequence of the gastric pathogen *Helicobacter pylori*. Nature (London) **388**, 539–547
6 Cheong, T. K. and Oriel, P. J. (2000) Cloning of a wide-spectrum amidase from *Bacillus stearothermophilus* BR388 in *Escherichia coli* and marked enhancement of amidase expression using directed evolution. Enzyme Microb. Technol. **26**, 152–158
7 Pace, H. C. and Brenner, C. (2001) The nitrilase superfamily: classification, structure and function. Genome Biology **2**, reviews0001.1–0001.9
8 Mahenthiralingam, E., Draper, P., Davis, E. O. and Colston, M. J. (1993) Cloning and sequencing of the gene which encodes the highly inducible acetamidase of *Mycobacterium smegmatis*. J. Gen. Microbiol. **139**, 575–583
9 Stevenson, D. E., Feng, R., Dumas, F., Groleau, D., Mihoc, A. and Storer, A. C. (1992) Mechanistic and structural studies on *Rhodococcus* ATCC 39484 nitrilase. Biotechnol. Appl. Biochem. **15**, 283–302
10 Arnaud, A., Galzy, P. and Jallageas, J. C. (1976) Nitrilase activity in several bacteria. C. R. Acad. Sci. Hebd. Seances Acad. Sci. D. **283**, 571–573

11 Harper, D. B. (1977) Fungal degradation of aromatic nitriles. Enzymology of C–N cleavage by *Fusarium solani*. Biochem. J. **167**, 685–692
12 Thimann, K. V. and Mahadevan, S. (1964) Nitrilase. Occurrence, preparation, and general properties of the enzyme. Arch. Biochem. Biophys. **105**, 133–141
13 Pekarsky, Y., Campiglio, M., Siprashvili, Z., Druck, T., Sedkov, Y., Tillib, S., Draganescu, A., Wermuth, P., Rothman, J. H., Huebner, K. et al. (1998) Nitrilase and Fhit homologs are encoded as fusion proteins in *Drosophila melanogaster* and *Caenorhabditis elegans*. Proc. Nat. Acad. Sci. U.S.A. **95**, 8744–8749
14 Pace, H. C., Hodawadekar, S. C., Draganescu, A., Huang, J., Bieganowski, P., Pekarsky, Y., Croce, C. M. and Brenner, C. (2000) Crystal structure of the worm NitFhit Rosetta Stone protein reveals a Nit tetramer binding two Fhit dimers. Curr. Biol. **10**, 907–917
15 Bork, P. and Koonin, E. V. (1994) A new family of carbon-nitrogen hydrolases. Protein Sci. **3**, 1344–1346
16 Novo, C., Tata, R., Clemente, A. and Brown, P. R. (1995) *Pseudomonas aeruginosa* aliphatic amidase is related to the nitrilase/cyanide hydratase enzyme family and Cys166 is predicted to be the active site nucleophile of the catalytic mechanism. FEBS Lett. **367**, 275–279
17 Farnaud, S., Tata, R., Sohi, M. K., Wan, T., Brown, P. R. and Sutton, B. J. (1999) Evidence that cysteine-166 is the active-site nucleophile of *Pseudomonas aeruginosa* amidase: crystallization and preliminary X-ray diffraction analysis of the enzyme. Biochem. J. **340**, 711–714
18 Brown, J. E., Brown, P. R. and Clarke, P. H. (1969) Butyramide-utilizing mutants of *Pseudomonas aeruginosa* 8602 which produce an amidase with altered substrate specificity. J. Gen. Microbiol. **57**, 273–285
19 Brown, J. E. and Clarke, P. H. (1970) Mutations in a regulator gene allowing *Pseudomonas aeruginosa* 8602 to grow on butyramide. J. Gen. Microbiol. **64**, 329–342
20 Brown, P. R. and Clarke, P. H. (1972) Amino acid substitution in an amidase produced by an acetanilide-utilizing mutant of *Pseudomonas aeruginosa*. J. Gen. Microbiol. **70**, 287–298
21 Betz, J. L. and Clarke, P. H. (1972) Selective evolution of phenylacetamide-utilizing strains of *Pseudomonas aeruginosa*. J. Gen. Microbiol. **73**, 161–174
22 Tata, R., Marsh, P. and Brown, P. R. (1994) Arg-188 and Trp-144 are implicated in the binding of urea and acetamide to the active site of the amidase from *Pseudomonas aeruginosa*. Biochim. Biophys. Acta **1205**, 139–145
23 Yoneda, T., Komooka, H. and Umeyama, H. (1997) A computer modelling study of the interaction between tissue factor pathway inhibitor and blood coagulation factor Xa. J. Protein Chem. **16**, 597–605
24 Ogata, K. and Umeyama, H. (1997) Prediction of protein side-chain conformations by principal component analysis for fixed main-chain atoms. Protein Eng. **10**, 353–359
25 Ogata, K. and Umeyama, H. (1998) The role played by environmental residues on sidechain torsional angles within homologous families of proteins: a new method of sidechain modelling. Proteins: Struct., Funct., Genet. **31**, 355–369
26 Peitsch, M. C. (1995) Protein modelling by E-mail. Bio/Technology **13**, 658–660
27 Peitsch, M. C. (1996) ProMod and Swiss-Model: Internet-based tools for automated comparative protein modelling. Biochem. Soc. Trans. **24**, 274–279
28 Guex, N. and Peitsch, M. C. (1997) SWISS-MODEL and the Swiss-PdbViewer: an environment for comparative protein modelling. Electrophoresis **18**, 2714–2723
29 Peitsch, M. C. and Guex, N. (1997) Large-scale comparative protein modelling. In Proteome Research: New Frontiers in Functional Genomics (Wilkins, M. R., Williams, K. L., Appel, R. O. and Hochstrasser, D. F., eds.), pp. 177–186, Springer
30 Laskowski, R. A., McArthur, M. W., Moss, D. S. and Thornton, J. M. (1993) PROCHECK: a program to check the stereochemical quality of protein structures. J. Appl. Crystallogr. **26**, 283–291
31 Flores, T. P., Moss, D. S. and Thornton, J. M. (1994) An algorithm for automatically generating protein topology cartoons. Protein Eng. **7**, 31–37
32 Katchalski-Katzir, E., Shariv, I., Eisenstein, M., Friesem, A. A., Aflalo, C. and Vakser, I. A. (1992) Molecular surface recognition: determination of geometric fit between proteins and their ligands by correlation techniques. Proc. Nat. Acad. Sci. U.S.A. **89**, 2195–2199
33 Vakser, I. A. and Aflalo, C. (1994) Hydrophobic docking: a proposed enhancement to molecular recognition techniques. Proteins: Struct., Funct., Genet. **20**, 320–329
34 Vakser, I. A. (1995) Protein docking for low-resolution structures. Protein Eng. **8**, 371–377
35 Vakser, I. A. (1996) Low-resolution docking: prediction of complexes for underdetermined structures. Biopolymers **39**, 455–464
36 Rodriguez, R., Chinea, G., Lopez, N., Pons, T. and Vriend, G. (1998) Homology modelling, model and software evaluation: three related resources. Bioinformatics **14**, 523–528
37 Kelly, M. and Clarke, P. H. (1962) An inducible amidase produced by a strain of *Pseudomonas aeruginosa*. J. Gen. Microbiol. **27**, 305–316
38 Smith, P. F. and Clarke, P. H. (1975) Catabolite repression of *Pseudomonas aeruginosa* amidase: the effect of carbon source on amidase synthesis. J. Gen. Microbiol. **90**, 81–90
39 Reference deleted
40 Gregoriou, M., Brown, P. R. and Tata, R. (1977) *Pseudomonas aeruginosa* mutants resistant to urea inhibition of growth on acetanilide. J. Bacteriol. **132**, 377–384
41 Cornish-Bowden, A. (1995) Analysis of Enzyme Kinetic Data, Oxford University Press, Oxford
42 Martin, A. C., MacArthur, M. W. and Thornton, J. M. (1997) Assessment of comparative modelling in CASP2. Proteins: Struct., Funct., Genet. (Suppl. 1), 14–28
43 Marchler-Bauer, A., Levitt, M. and Bryant, S. H. (1997) A retrospective analysis of CASP2 threading predictions. Proteins: Struct., Funct., Genet. (Suppl. 1), 83–91
44 Lesk, A. M. (1997) CASP2: report on *ab initio* predictions. Proteins: Struct., Funct., Genet. (Suppl. 1), 151–166
45 Vakser, I. A. (1996) Long-distance potentials: an approach to the multiple-minima problem in ligand-receptor interaction. Protein Eng. **9**, 37–41
46 Nakai, T., Hasegawa, T., Yamashita, E., Yamamoto, M., Kumasaka, T., Ueki, T., Nanba, H., Ikenaka, Y., Takahashi, S., Sato, M. and Tsukihara, T (2000) Crystal structure of N-carbamyl-D-amino acid amidohydrolase with a novel catalytic framework common to amidohydrolases. Structure (London) **8**, 729–739
47 Karmali, A., Tata, R. and Brown, P. R. (2000) Substitution of Glu-59 by Val in amidase from *Pseudomonas aeruginosa* results in a catalytically inactive enzyme. Mol. Biotechnol. **16**, 5–16
48 Gregoriou, M. and Brown, P. R. (1979) Inhibition of the aliphatic amidase from *Pseudomonas aeruginosa* by urea and related compounds. Eur. J. Biochem. **96**, 101–108
49 Woods, M. J., Edgeworth, M. A. and Orsi, B. A. (1975) Studies on the active site of the amidase from *Pseudomonas aeruginosa*. Biochem. Soc. Trans. **3**, 1216–1219
50 Karmali, A., Pacheco, R., Tata, R. and Brown, P. R. (2001) Substitutions of Thr-103-Ile and Trp-138-Gly in amidase from *Pseudomonas aeruginosa* are responsible for altered kinetic properties and enzyme instability. Mol. Biotechnol. **17**, 201–212

Received 22 November 2001/26 March 2002; accepted 15 April 2002
Published as BJ Immediate Publication 15 April 2002, DOI 10.1042/BJ20011714